

Gyroscopic effects in interference of matter waves

Oleg I. Tolstikhin¹, Toru Morishita², and Shinichi Watanabe²

¹*Russian Research Center “Kurchatov Institute”,
Kurchatov Square 1, Moscow 123182, Russia*

²*Department of Applied Physics and Chemistry,
University of Electro-Communications,
1-5-1, Chofu-ga-oka, Chofu-shi, Tokyo 182-8585, Japan*

(Dated: November 21, 2018)

Abstract

A new gyroscopic interference effect stemming from the Galilean translational factor in the matter wave function is pointed out. In contrast to the well-known Sagnac effect that stems from the geometric phase and leads to a shift of interference fringes, this effect causes slanting of the fringes. We illustrate it by calculations for two split cigar-shaped Bose-Einstein condensates under the conditions of a recent experiment, see Y. Shin *et al.*, Phys. Rev. Lett. **92**, 050405 (2004). Importantly, the measurement of slanting obviates the need of a third reference cloud.

PACS numbers: 03.75.-b, 03.75.Dg, 03.75.Nt, 03.65.Vf

From the spinning mass gyroscope to modern light and matter wave interferometers is a spectacular evolution in man's technology for sensing a change in orientation. From navigation of ships and spacecrafts to studying the seismic motion of tectonic plates, the applications of gyro keep motivating further scientific and engineering progress in the field. It thus merits to point out in this Communication a new gyroscopic interference effect that stems from the Galilean translational factor in the matter wave function.

The rotation-sensitive interference experiments have a long history. A rotation-induced difference in optical paths for two light beams counter-propagating around a closed contour causes a shift of the interference fringes, which was conceived by Sagnac as a subject of interferometry [1]. This first demonstration of the Sagnac effect was performed on a rotating table. Soon afterward, the first measurement of the Earth's rotation was done by Michelson and Gale [2] with a very large stationary light interferometer operating on the same principle. The advent of lasers ensued a rapid progress in the optical measurements of the Sagnac effect and culminated with the creation of miniature ring laser gyros currently in use for navigation, see a review [3]. The Sagnac effect for matter waves was theoretically predicted in [4]. The result can be obtained by changing light to matter via the substitution $\hbar\omega = mc^2$ into the expression for the Sagnac phase shift. The advantage of matter waves is in the possibility of considerably down-sizing the interferometer owing to the reduced wavelength. The effect was demonstrated experimentally first with neutrons [5, 6] and later with neutral atoms [7] and charged particles (electrons) [8]. There is also a suggestion for hybridizing light and matter waves by way of polaritons [9]. Highest precision and stability to date were achieved with atom interferometers: on a rotating table, at rates of rotation of the order of Earth's rate [10], and with stationary apparatus, detecting the rotation of Earth [11]. It can hardly be overemphasized that Bose-Einstein condensates (BECs) provide a new type of matter wave sources. Their high brightness and coherence make them to matter wave interferometry what lasers are to optical interferometry. A single measurement of interference with BECs should suffice to determine the rotation velocity; this paper explores BEC as a gyroscope for this specific reason apart from a further miniturization. The first demonstration of interference between two BECs was reported in [12]. Interference of BECs in lattices was also observed [13, 14]. Recently, two cigar-shaped BECs in a double-well potential were made to interfere keeping the relative phase of atomic clouds under control [15]. The authors conclude: "Propagating the separated condensates along a microfabricated wave guide prior

to phase readout would create an atom interferometer with an enclosed area, and hence with rotation sensitivity”. Thus rotation-sensitive BEC interferometers should become available soon.

In all the above experiments, done and planned, rotation reveals itself via a shift of interference fringes owing to the Sagnac effect. In this paper we show that there is another effect that leads to slanting of the fringes.

As noted above, the discussion to follow deals with BEC as a bright source of matter waves, so that we base our consideration on the Gross-Pitaevskii (GP) equation [16], but the argumentation applies also to a dilute atomic cloud [that is including the limit of $\beta = 0$ in Eq. (1)]. The phenomenon we present here is thus of a rather general nature, but our specific reference to BEC as a matter wave source inevitably leads us to include dynamical effects of the nonlinear term. The positive internal pressure expressed by the nonlinear term is conducive to rapid expansion of the system when the trap is switched off. The GP equation in a rotating reference frame reads

$$i\hbar \frac{\partial \psi(\mathbf{r}, t)}{\partial t} = \left[\frac{\mathbf{p}^2}{2m} - \boldsymbol{\Omega} \cdot \mathbf{l} + V(\mathbf{r}, t) + \beta |\psi(\mathbf{r}, t)|^2 \right] \psi(\mathbf{r}, t). \quad (1)$$

Here $\boldsymbol{\Omega}$ is the angular velocity of rotation, $V(\mathbf{r}, t)$ is the trap potential, $\beta = 4\pi N\hbar^2 a/m$ is the coupling constant, where m , a , and N are the atomic mass, scattering length, and the number of atoms, respectively, and the order parameter $\psi(\mathbf{r}, t)$ is normalized to unity. We shall assume that $\boldsymbol{\Omega}$ is small and does not depend on time. Let us consider a simple *gedanken* experiment to detect rotation, first with the aid of an approximate representation of the experimental steps, and then Eq. (1) will be numerically solved subject to realistic experimental conditions. The experiment proceeds in four steps, see Fig. 1: (1) preparation of the initial state, which we assume to be the ground state of a BEC in a single-well trap, (2) coherent splitting of the BEC into two or more components by deforming the potential into several separated traps, (3) independent transportation of the components along some paths by varying the positions of the traps, and (4) switching off the potential and observation of the interference pattern when the different components begin to overlap as a result of their free expansion. Assuming that steps 2 and 3 are done adiabatically slowly the effects of rotation on the interference pattern can be deduced analytically. The *adiabaticity* means that the system remains in the ground state at each moment; we will return to this point in the discussion of numerical results. During step 3 the solution to Eq. (1) can be decomposed

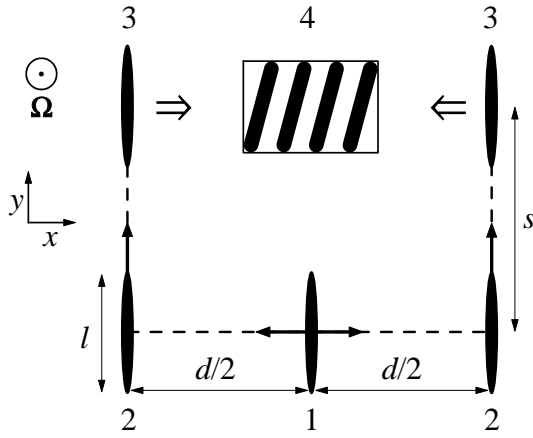


FIG. 1: General scheme of a rotation-sensitive interference experiment with BEC. A BEC, initially in a single cigar-shaped trap (1), is split coherently in the transverse direction into two parts (2), which are then moved in the longitudinal direction and released to expand freely (3). The interference pattern (4) is obtained by measuring the atomic density when the clouds begin to overlap.

as

$$\psi(\mathbf{r}, t) = \sum_n \psi_n(\mathbf{r}, t), \quad (2)$$

where the overlap of the different components $\psi_n(\mathbf{r}, t)$ is geometrically marginal but physically non-negligible due to tunneling. The position of the n -th component is given by

$$\mathbf{a}_n(t) = \frac{\langle \psi_n^*(\mathbf{r}, t) \mathbf{r} \psi_n(\mathbf{r}, t) \rangle_n}{\langle \psi_n^*(\mathbf{r}, t) \psi_n(\mathbf{r}, t) \rangle_n}, \quad (3)$$

where $\langle \dots \rangle_n$ denotes integration over the region occupied by the n -th trap. In this region $V(\mathbf{r}, t) = V_n(\mathbf{r} - \mathbf{a}_n(t), t)$, where $V_n(\mathbf{r}, t)$ defines the shape of the n -th trap. If $\mathbf{a}_n(t)$ and $V_n(\mathbf{r}, t)$ are slowly varying functions of t , in the adiabatic approximation we obtain

$$\psi_n(\mathbf{r}, t) = \exp \left[-i\hbar^{-1} \int^t \mu(t') dt' + i\gamma_n(t) \right] \phi_n(\mathbf{r}; t), \quad (4)$$

where $\mu(t)$ and $\phi_n(\mathbf{r}; t)$ constitute the ground state solution of the stationary equation

$$\left[\frac{\mathbf{p}^2}{2m} - \boldsymbol{\Omega} \cdot \mathbf{l} + V_n(\mathbf{r} - \mathbf{a}_n(t), t) + \beta |\phi_n(\mathbf{r}; t)|^2 - \mu(t) \right] \phi_n(\mathbf{r}; t) = 0 \quad (5)$$

that depends on t as a parameter, and $\gamma_n(t)$ is the geometric phase [17],

$$\gamma_n(t) = i \int^t \frac{\langle \phi_n^*(\mathbf{r}; t') \partial \phi_n(\mathbf{r}; t') / \partial t' \rangle_n}{\langle \phi_n^*(\mathbf{r}; t') \phi_n(\mathbf{r}; t') \rangle_n} dt'. \quad (6)$$

Note that the chemical potential $\mu(t)$ does not depend on n and corresponds to the ground state of the whole system, which assumes that equilibrium is attained at each instant of

time via tunneling between the components [18]. Our key observation is that the solution to Eq. (5) can be presented in the form

$$\mu(t) = \bar{\mu}(t) + O(\Omega^2), \quad (7a)$$

$$\phi_n(\mathbf{r}; t) = \exp [i\hbar^{-1}m\mathbf{v}_n(t) \cdot \mathbf{r}] \bar{\phi}_n(\mathbf{r} - \mathbf{a}_n(t); t) + O(\Omega^2), \quad (7b)$$

where $\bar{\mu}(t)$ and $\bar{\phi}_n(\mathbf{r}; t)$ constitute the ground state solution of

$$\left[\frac{\mathbf{p}^2}{2m} - \boldsymbol{\Omega} \cdot \mathbf{l} + V_n(\mathbf{r}, t) + \beta |\bar{\phi}_n(\mathbf{r}; t)|^2 - \bar{\mu}(t) \right] \bar{\phi}_n(\mathbf{r}; t) = 0, \quad (8)$$

and $\mathbf{v}_n(t) = \boldsymbol{\Omega} \times \mathbf{a}_n(t)$. The exponent in Eq. (7b) is the Galilean translational factor; it accounts for the fact that the n -th component moves with the velocity $\mathbf{v}_n(t)$ with respect to a non-rotating inertial frame whose origin coincides with that of the rotating frame. The solution of Eq. (8) may have a nonzero phase $O(\Omega)$ which, however, disappears if the potential $V_n(\mathbf{r}, t)$ becomes axially symmetric about the direction of $\boldsymbol{\Omega}$. The validity of Eqs. (7) can be confirmed for the special case of a harmonic oscillator trap. Substituting into Eqs. (5) and (8) $V_n(\mathbf{r}, t) = V_{\text{HO}}(\mathbf{r}) = \frac{1}{2} m \mathbf{r}^T \hat{\omega}^2 \mathbf{r}$ and $\mathbf{a}_n(t) = \mathbf{a}$, where $\hat{\omega} = \text{diag}(\omega_x, \omega_y, \omega_z)$ is a diagonal matrix, \mathbf{r} is treated as a column, and \mathbf{r}^T denotes the corresponding row, one can obtain an exact relation between the solutions to these equations,

$$\mu = \bar{\mu} - \frac{m\mathbf{u}^2}{2} + V_{\text{HO}}(\mathbf{b} - \mathbf{a}), \quad (9a)$$

$$\phi(\mathbf{r}) = \exp [i\hbar^{-1}m\mathbf{u} \cdot \mathbf{r}] \bar{\phi}(\mathbf{r} - \mathbf{b}), \quad (9b)$$

where $\mathbf{u} = \boldsymbol{\Omega} \times \mathbf{b}$ and $\mathbf{b} = (\hat{\omega}^2 + \boldsymbol{\Omega}\boldsymbol{\Omega}^T - \Omega^2)^{-1} \hat{\omega}^2 \mathbf{a}$. It can be easily seen that $\mathbf{b} = \mathbf{a} + O(\Omega^2)$, so the result (9) is in agreement with Eqs. (7). From Eqs. (3), (6), and (7b) we find [4]

$$\gamma_n(t) = \hbar^{-1}m \int^{\mathbf{a}_n(t)} \boldsymbol{\Omega} \times \mathbf{a} \cdot d\mathbf{a}, \quad (10)$$

where the integral is calculated along the path traced by the vector $\mathbf{a}_n(t)$. Summarizing, we can specify Eq. (2) as follows

$$\psi(\mathbf{r}, t) = \exp \left[-i\hbar^{-1} \int^t \bar{\mu}(t') dt' \right] \sum_n \exp [i\gamma_n(t) + i\hbar^{-1}m\mathbf{v}_n(t) \cdot \mathbf{r}] \bar{\phi}_n(\mathbf{r} - \mathbf{a}_n(t); t). \quad (11)$$

This function provides an initial state for free expansion during step 4. The resulting interference pattern depends on the phases of the components in Eq. (11), and hence is sensitive to rotation. A difference between the geometric phases leads to a shift of the interference

fringes; this is the Sagnac effect. The Galilean factors introduce an additional phase difference; this phase is inhomogeneous, which causes a deformation of the interference pattern. There is also a third effect: the interference pattern rotates with respect to the rotating frame, similarly to the rotation of the plane of motion of the Foucault pendulum. It is the last two effects that may result in slanting of the fringes, as is shown below, and their manifestation should be clearly distinguished from the Sagnac effect.

We illustrate this general consideration by calculations for a two-dimensional system modeling the experiment discussed above. Number as well as phase fluctuations in BECs are supposedly problematic in measuring a shift of the fringes, but do not affect their slanting. So we use the GP equation without explicit representation of the fluctuations [18]. The results reported below were obtained from Eq. (1) directly, with no approximation or ansatz to the GP equation, by propagating the solution in time in a finite spatial rectangle $-d \leq x \leq d$, $-l/2 \leq y \leq l/2$, with the condition $\psi(x, y, t) = 0$ on its boundaries. A BEC containing $N = 10^4$ atoms ^{23}Na ($m = 3.82 \times 10^{-26}$ kg, $a = 2.75 \times 10^{-3}$ μm) is initially in a single-well trap, see Fig. 1. The trap is formed by a Gaussian potential $V_0(x) = -U_0 \exp(-\frac{1}{2}m\omega^2 x^2/U_0)$, in the x direction, and zero boundary conditions at $y = \pm l/2$, in the y direction, with the trap depth $U_0 = h \times 5$ kHz, frequency $\omega = 2\pi \times 615$ Hz, and length $l = 23$ μm . In the first stage of the calculations, the ground state in the trap is obtained by propagating Eq. (1) in imaginary time. The atomic density in this state has a cigar-like shape with the width 6.8 μm on the level of 1% of the maximum value. In the second stage, the atomic cloud is split in the x direction into two equal cigar-shaped parts by varying the potential according to $V(x, t) = f(t)[V_0(x - vt) + V_0(x + vt)]$ with a constant velocity v during time $\tau_x = 5$ ms, where the factor $f(t)$ is introduced to preserve trap's depth at each moment equal to U_0 , with $f(0) = 1/2$ and $f(\tau_x) \approx f(\infty) = 1$. The final distance between the cigars is $d = 2v\tau_x = 13$ μm , and their width is 5.6 μm , so to a very good approximation (i) cigars do not overlap, and (ii) the zero boundary conditions at $x = \pm d$ do not affect the solution of Eq. (1). Similar coherent splitting of a cigar-shaped BEC into two parts was realized in a recent experiment [15]. The above values of ω , U_0 , d , and τ_x coincide with the values of these parameters in [15], but in order to facilitate the calculations the cigar length l , and hence the number of atoms N , are taken to be equal to about one tenth of their values in [15]. In the third stage, the cigars are transported in the y direction with the same constant velocity v during time τ_y . This is done by introducing into the Hamiltonian in Eq. (1) an

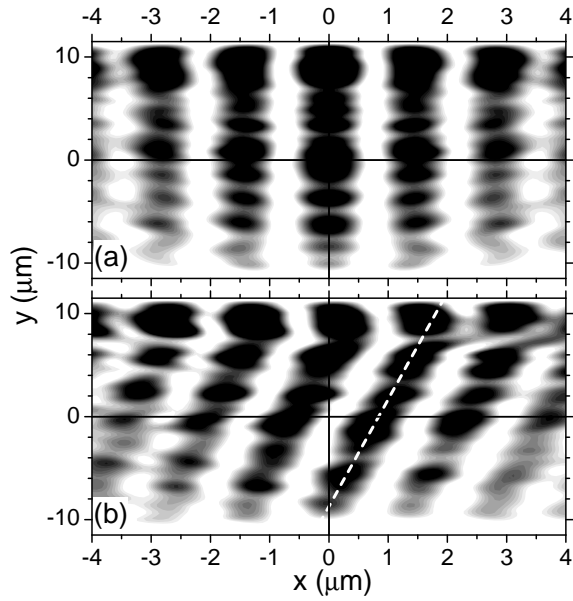


FIG. 2: An interference pattern obtained by simulation of the experiment shown in Fig. 1 under the conditions similar to that realized recently [15] without rotation (a) and with rotation (b). In the latter case the interference fringes are shifted (the Sagnac effect) and slanted; the white dashed line is a fit to the central fringe according to Eq. (15).

additional term $-vp_y$. The transportation distance $s = v\tau_y$ is chosen to be equal to cigar's length, $s = 23 \mu\text{m}$, which corresponds to $\tau_y = 17.7$ ms. Finally, in the fourth stage, the potential is switched off and the atomic clouds are allowed to expand freely during time $\tau = 1$ ms. The boundaries at $x = \pm d$ still do not affect the results because this time is too short for the waves reflected from them could reach the central region $|x| \leq 4 \mu\text{m}$, where the interference pattern is observed. The calculations were done without rotation, $\Omega = 0$, and with rotation for $\Omega = 10^{-2} \times \omega$; the results are shown in Fig. 2. Because of finiteness of the velocity v , some oscillations of the atomic density are excited during the splitting and transportation processes that distort the interference pattern. Indeed, because of the cigar shape, the density oscillation along the longitudinal axis has a low frequency and is susceptible to nonadiabatic excitations.

We have repeated the calculations for 20 times slower motion ($\tau_x = 100$ ms, $\tau_y = 354$ ms) with the same values of all the other parameters, see Fig. 3. This situation is much closer to the adiabatic regime, and the interference pattern in this case is perfectly smooth. As can be seen from the figures, the question of adiabaticity is of considerable importance.

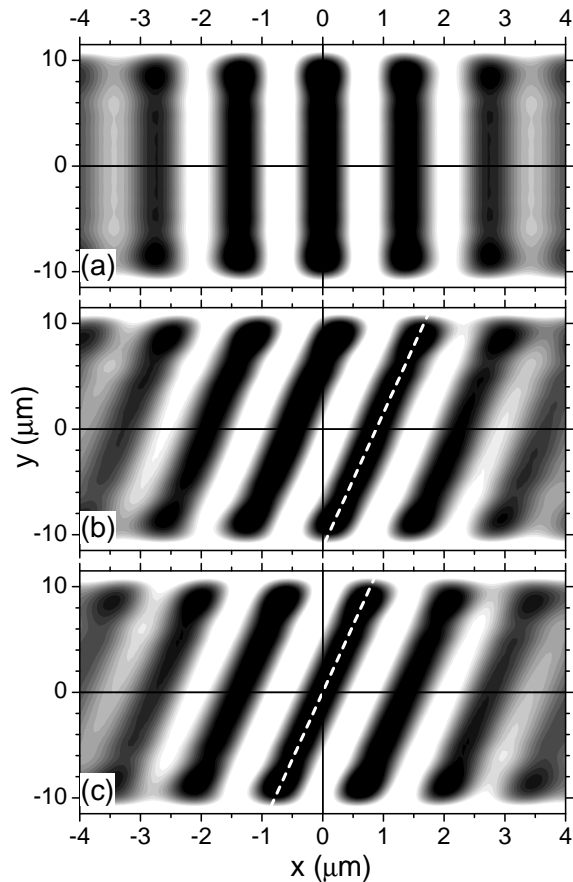


FIG. 3: (a) and (b): similar to Fig. 2, but for 20 times slower motion during steps 2 and 3 in Fig. 1. (c): same as in (b), but skipping step 3; there is no Sagnac shift in this case, but slanting remains unchanged.

Elementary excitations caused by nonadiabatic processes would quite generally complicate the interference pattern and make the identification of fringes difficult. Hence the experiment must be conducted slow enough so that energy imparted to the BEC should not exceed the excitation threshold. Anyway, in both cases one can clearly see that in the presence of rotation the interference fringes are shifted and slanted. We note that in real experiment the phase shift may suffer from uncontrollable offset from run to run while the slanting angle is known *a priori* to be zero in the absence of rotation. An interesting possibility of observing the effect of slanting is thus assured by the very manifestation of interference fringes.

To interpret these results, following [15] we assume that the expansion can be described by Eq. (1) with $\beta = 0$. In the adiabatic regime, the initial condition for this equation has

the form (11). Then for the atomic density in the interference region we obtain

$$n(x, y, t) = N|\psi(x, y, t)|^2 \propto 1 + \cos\left(\frac{md}{\hbar t}x' - \gamma_S - \frac{\gamma_G}{l}y'\right), \quad (12)$$

where (x, y) and (x', y') are the coordinates of the point of observation in the rotating and non-rotating reference frames, respectively, and the time t is measured from the moment of release. The first term in the argument of the cosine function in Eq. (12) corresponds to free expansion in the x direction of two point-like sources initially located at $x = \pm d/2$. The second term comes from the geometric phases in Eq. (11) and is given by

$$\gamma_S = \hbar^{-1}m\Omega ds. \quad (13)$$

The third term, where

$$\gamma_G = \hbar^{-1}m\Omega dl, \quad (14)$$

comes from the Galilean factors in Eq. (11). Substituting into Eq. (12) $x' = x \cos(\Omega t) - y \sin(\Omega t) = x - \Omega t y + O(\Omega^2)$ and $y' = x \sin(\Omega t) + y \cos(\Omega t) = y + O(\Omega)$, we obtain

$$n(x, y, t) \propto 1 + \cos\left(\frac{md}{\hbar t}x - \gamma_S - \frac{2\gamma_G}{l}y\right). \quad (15)$$

Thus in the presence of rotation the interference fringes are shifted by γ_S , which is the Sagnac effect, and slanted, with the phase shift between their upper and lower ends ($y = \pm l/2$) equal to $2\gamma_G$. These simple equations work surprisingly well. Indeed, according to Eq. (15) the spatial period of the fringes is $\lambda = h\tau/md = 1.35 \mu\text{m}$, which is very close to $\lambda^{\text{calc}} = 1.38 \mu\text{m}$ obtained by fitting the numerical results. From Eqs. (13) and (14) we have $\gamma_S = \gamma_G = 4.15$ (recall that in our case $s = l$). Fitting the position of the central fringe in Fig. 2(b) we obtain $\gamma_S^{\text{calc}} = 3.85$ and $\gamma_G^{\text{calc}} = 5.07$; similarly from Fig. 3(b) we find $\gamma_S^{\text{calc}} = 4.04$ and $\gamma_G^{\text{calc}} = 4.13$.

To conclude, we have discussed a gyroscopic effect that stems from the Galilean translational factor. In contrast to the Sagnac effect that leads to a homogeneous shift of interference fringes, the Galilean phase causes an inhomogeneous shift between the ends of the fringes, i.e., their slanting. For the situation considered (cigar-shaped geometry with $s \sim l$) both effects are of the same order of magnitude. However, to produce a shift two steps are needed, transverse separation and longitude transportation, while for slanting the first step is sufficient, see Fig. 3(c). Another important difference is that the Sagnac phase is subject to uncertainty due to a possible asymmetry between the traps and uncontrollable

variations from run to run of the experiment which need to be compensated for by using a third reference cloud, while slanting is not affected by these factors.

This work was supported in part by a Grant-in-Aid for Scientific Research (C) from the Ministry of Education, Culture, Sports, Science and Technology, Japan, and also in part by the 21st Century COE program on “Coherent Optical Science”. TM was also supported in part by a Grant-in-Aid for Young Scientist (B) from Japan Society for the Promotion of Science and by a financial aid from the Matsuo Foundation.

-
- [1] G. Sagnac, C. R. Acad. Sci. **157**, 708 (1913); **157**, 1410 (1913); J. Phys. (Paris) **4**, 177 (1914).
 - [2] A. A. Michelson and H. G. Gale, assisted by F. Pearson, Astrophys. J. **61**, 140 (1925).
 - [3] W. W. Chow, J. Gea-Banaacloche, L. M. Pedrotti, V. E. Sanders, W. Schleich, and M. O. Scully, Rev. Mod. Phys. **57**, 61 (1985).
 - [4] L. A. Page, Phys. Rev. Lett. **35**, 543 (1975).
 - [5] S. A. Werner, J.-L. Staudenmann, and R. Colella, Phys. Rev. Lett. **42**, 1103 (1979).
 - [6] D. K. Atwood, M. A. Horne, C. G. Shull, and J. Arthur, Phys. Rev. Lett. **52**, 1673 (1984).
 - [7] F. Riehle, Th. Kisters, A. Witte, J. Helmcke, and Ch. J. Bordé, Phys. Rev. Lett. **67**, 177 (1991).
 - [8] F. Hasselbach and M. Nicklaus, Phys. Rev. A **48**, 143 (1993).
 - [9] F. Zimmer and M. Fleischhauer, Phys. Rev. Lett. **92**, 253201 (2004).
 - [10] A. Lenef, T. D. Hammond, E. T. Smith, M. S. Chapman, R. A. Rubenstein, and D. E. Pritchard, Phys. Rev. Lett. **78**, 760 (1997).
 - [11] T. L. Gustavson, P. Bouyer, and M. A. Kasevich, Phys. Rev. Lett. **78**, 2046 (1997); T. L. Gustavson, A. Landragin, and M. A. Kasevich, Class. Quantum Grav. **17**, 2385 (2000).
 - [12] M. R. Andrews, C. G. Townsend, H.-J. Miesner, D. S. Durfee, D. M. Kurn, and W. Ketterle, Science **275**, 637 (1997).
 - [13] B. P. Anderson and M. A. Kasevich, Science **281**, 1686 (1998).
 - [14] M. Greiner, I. Bloch, O. Mandel, T. W. Hänsch, and T. Esslinger, Phys. Rev. Lett. **87**, 160405 (2001); C. Orzel, A. K. Tuchman, M. L. Fenselau, M. Yasuda, and M. A. Kasevich, Science **291**, 2386 (2001); Z. Hadzibabic, S. Stock, B. Battelier, V. Bretin, and J. Dalibard, Phys. Rev. Lett. **93**, 180403 (2004).

- [15] Y. Shin, M. Saba, T. A. Pasquini, W. Ketterle, D. E. Pritchard, and A. E. Leanhardt, Phys. Rev. Lett. **92**, 050405 (2004).
- [16] F. Dalfovo, S. Giorgini, L. P. Pitaevskii, and S. Stringari, Rev. Mod. Phys. **71**, 463 (1999).
- [17] M. V. Berry, Proc. R. Soc. Lond. A **392**, 45 (1984).
- [18] The assumed equipartition $N_1 = N_2 = N/2$ would forbid variation in number of atoms in either well. In an actual implementation, departures should occur. In this connection, it is worth pointing out that the Josephson junction as well as the self-trapping are observed and discussed in M. Albiez, R. Gati, J. Fölling, S. Hunsmann, M. Cristiani, and M. K. Oberthaler, Phys. Rev. Lett. **95**, 010402 (2005). These should not overshadow the major effect discussed in the text.